The Seventh International Colloquium on Bluff Body Aerodynamics and Applications (BBAA7)
Shanghai, China; September 2-6, 2012

Wind pressure characteristics of square prism under non-stationary wind in multiple-fan wind tunnel

Yoshiyuki Tatewaki[a], Jun Kanda[b], Hitomisu Kikitsu[c], Yuan-Lung Lo[d]

[a] *Daiwa House Industry Co., Ltd., Kita, Osaka, Japan*
[b] *Nihon University, Chiyoda, Tokyo, Japan*
[c] *Building Research Institute, Tsukuba, Ibaraki, Japan*
[d] *University of Tokyo, Kashiwa, Chiba, Japan*

ABSTRACT: Statistical analyses of tornado-induced damages in Japan have been conducted and compared with Fujita Tornado Damage Scale for determining the parameters of tornado model. Based on determined parameters, tornados were scaled down and reproduced by tornado generator facilities for comparison with observed statistics. Then, by utilizing multiple-fan wind tunnel, non-stationary flow of tornado was simulated and wind pressure measurement of prism models under such flow was conducted to evaluate the distributions of wind pressure coefficients due to overshoot phenomenon observed in tornado-like wind velocities.

KEYWORDS: Tornado, Tornado model, Multiple-fan wind tunnel,
Tornado simulator, Non-stationary wind, Wind pressure characteristics

1 INTRODUCTION

Non-stationary winds induced by tornados have been investigated such as by Maeda et al ([5]) for overshoot phenomena of wind forces caused by gusty winds; by Ikeuchi et al ([2]) for the effect of wind direction changes. However, these investigations cannot be confirmed generally in the traditional turbulent boundary layer wind tunnels and many assumptions must be determined preliminarily. In this research, non-stationary wind direction change induced by tornados is focused. It is intended to clarify the effect on the prism models caused by such dramatic wind direction change by multiple-fan wind tunnel.

1.1 *General Instructions*

It was reported three casualties and one fully damaged building caused by gusty winds in Tokuno-jima, Kagoshima Prefecture on 11/18, 2012 ([8]). Generally speaking, the occurrence probability that tornado attacks one specific location is low and tornado-dependent wind resistant design for buildings is not provided in the current Japanese regulations. However, for nuclear power plants or long life structures, wind resistant design considering tornados that possess low occurrence probabilities must be considered. To include the observed tornado-induced damages in Japan, the practical tornado resistant design for important structures is essential and necessary.

In order to fully understand the tornado feature in Japan, including the wind speed profile and the wind direction change, the investigation is conducted as follows: (1) statistical studies on the recent tornado records for the specific virtual tornado model in Japan; (2) understanding the characteristics of tornado through reproducing tornado-like winds by tornado generator facilities; and (3) investigating the non-stationary effect of winds on prism models in a short period by utilizing multiple-fan wind tunnel in University of Tokyo ([7]).

2 PARAMETERS – *THEORETICAL TORNADO MODEL*

2.1 *Statistical Information of Tornado-induced Damage in Japan and Assumptions for Modeling*

Although plenty of reports or surveys have been carried out for investigation on tornado-induced damages in Japan, investigation items, such as damage path width or length, are judged subjectively based on the status of building damage appearances, which may sometimes results in significant biases for statistical studies. In order to avoid such data bias, this research utilized weather database since 1961 provided by Japan Meteorological Agency. The database includes all the tornado and downburst events. However, several assumptions are necessary for further investigations. The modeling of tornado in this research is assumed that counterclockwise Rankine tornado remains circular and moves constantly. And only horizontal wind speed component is investigated in this research.

2.2 *Time History and Occurrence Probability of Simulated Tornado Model*

Based on Fujita Tornado Damage Scale, Table 1 lists the recent records and the simulated models used in this research (VF). Applying the parameters of a simulated VF3 tornado in Table 1 as a Rankine tornado, Figure 1 shows the simulated time history and wind direction change. It is indicated that significant effects on structures can be considered resulted from the extremely high wind speed in the right side of the tornado and from the dramatic changes of wind speed and direction in a short period for the center of the tornado passing.

Table 1 Recent records and assumed tornado models

model	F scale	Wind speed (m/s)	movement (m/s)	radius (m)
Toyohashi	3	81	16.2	28.3
Mobara	3	81	20.9	80.0
Urawa	3	81	8.6	8.4
Saroma	3	81	28.8	30.2
Nobeoka	2	60	32.4	38.0
VF2	2	60	15.5	14.7
VF3	3	81	20.6	22.5
VF4	4	105	25.6	36.2
VF5	5	130	30.7	60.1

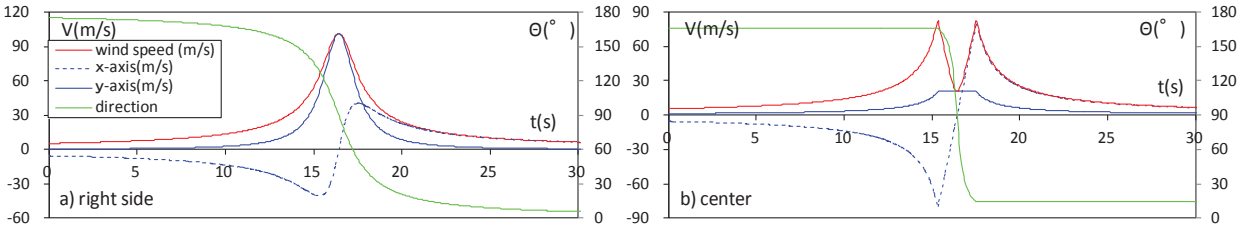

Figure 1 Wind speed and direction profile of assumed tornado model

Figure 2 shows the simulated parameters of tornado models in Table 1 and the ones suggested by American guideline, American National Standard for Estimating Tornado and Extreme Wind Characteristics at Nuclear Power Sites (ANSI/ANS-2.3-1983).

Comparing suggested tornado models by American standard and the simulated tornado models utilized in this research, it is known that the moving speed of the simulated one is 10% higher than American standard and the magnitude is only 25%. Based on this comparison, the simulated

tornado model specified in Japan is assumed F3 scale and the corresponding parameters are utilized for further experiments.

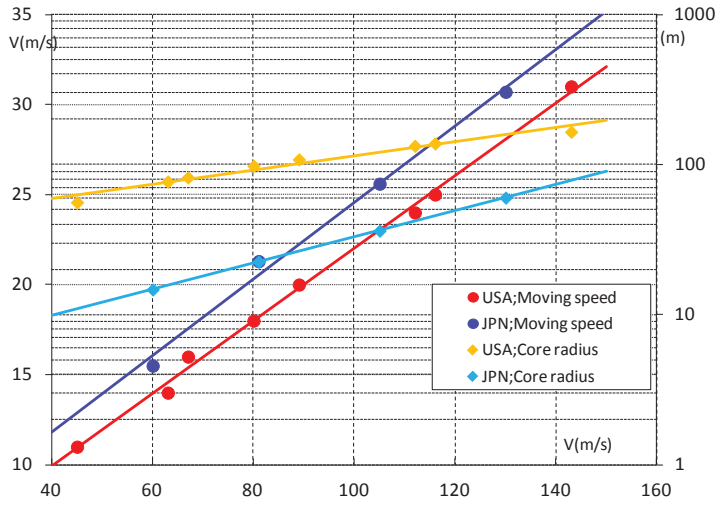

Figure 2 Comparison of assumed tornado models in Japan and suggested models by American standards

3 TORNADO REPRODUCTIONS BY TORNADO GENERATOR FACILITIES

To understand the characteristics of wind speed and wind direction changes of a tornado, a VF3 simulated tornado model mentioned in the previous section is simulated by the tornado generator facilities.

3.1 *Tornado Generator Facilities*

For the tornado generator facilities, the fan is hidden inside the main facility which can be driven by active control system to move constantly and straightly shown in Figure 3. 18 guide vans are set in the fan to generate rotary downward flows and the setting angle of vans tangent to the fan can be arbitrarily adjusted. The maximum moving speed of the main facility is 0.4m/sec. In this research, tornados with the setting angle of vans, 30°, and the rotation frequency of the fan, 8Hz, are generated for investigation of non-stationary wind flows. Sampling rate is 20Hz for 40 seconds for each sample.

Wind speed is measured from the center to the outer radius of a still simulated tornado. Figure 4 shows the wind speed profile along Z-Z axis of a still simulated tornado. The core radius is 100mm (R) and the tangent maximum wind speed is 4.29m/sec (V_m). However, the center of the simulated tornado is 10mm away from the centerline of the moving line of the experimental table.

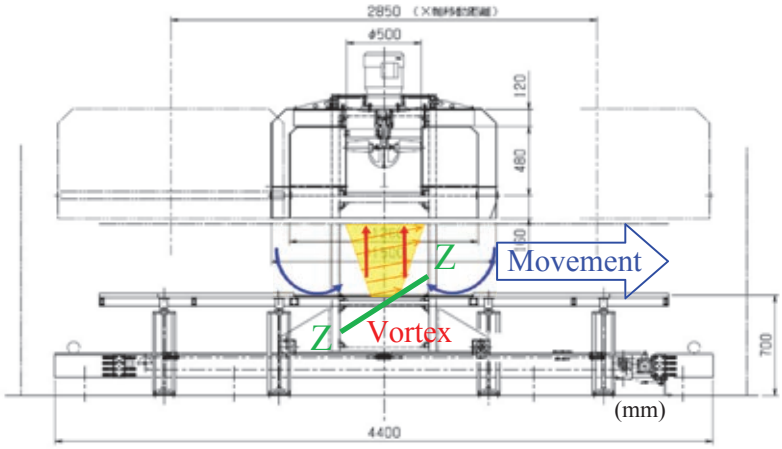

Figure 3 Tornado simulator with vortex generator

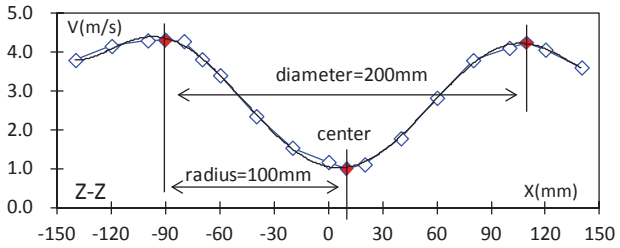

Figure 4 Wind speed distribution along Z-Z axis

3.2 *Characteristics of Wind Speed and Direction Changes of Tornado Winds*

Figure 5 shows the time histories of wind speeds and directions at the center of tornado and the right side of the moving path of the tornado when the moving speed is 0.1m/sec and 0.3m/sec (V_t). Wind speed measurements are conducted by I type hot-wire anemometers and Figure 5 shows the ensample average of 10 samples. From Figure 5, instead of Rankine tornado model, Shakeel's theoretical model ([4]) seems fit better to the experimental results (hereafter SA model). The formula to represent SA model are as follows.

Boundary layer thickness:

$$\delta(r') = \delta_0\left[1 - e^{-0.5r^2}\right] \tag{1-1}$$

Radial function:

$$r = {r'}/{r_{max}} \qquad \eta = {z}/{\delta} \tag{1-2}$$

T=tangential velocity component

$$T(\eta, r) = f(r) = 1.4\frac{V_{max}}{r}\left[1.0 - e^{-1.256r^2}\right] \tag{1-3}$$

W=vertical velocity component

$$W(\eta, r) = g(r) = 93.0r^3e^{-5r}V_{max} \qquad \eta > 1 \tag{1-4}$$

T=tangential velocity component

$$T(\eta, r) = f(r)[1 - e^{-\pi\eta}\cos(2b\pi\eta)] \quad (1\text{-}5)$$

R=radial velocity component

$$R(\eta, r) = f(r)[0.672e^{-\pi\eta}\sin\{(b+1)\pi\eta\}] \quad (1\text{-}6)$$

W=vertical velocity component

$$W(\eta, r) = g(r)[1 - e^{-\pi\eta}\cos(2b\pi\eta)] \qquad \eta \le 1 \quad (1\text{-}7)$$

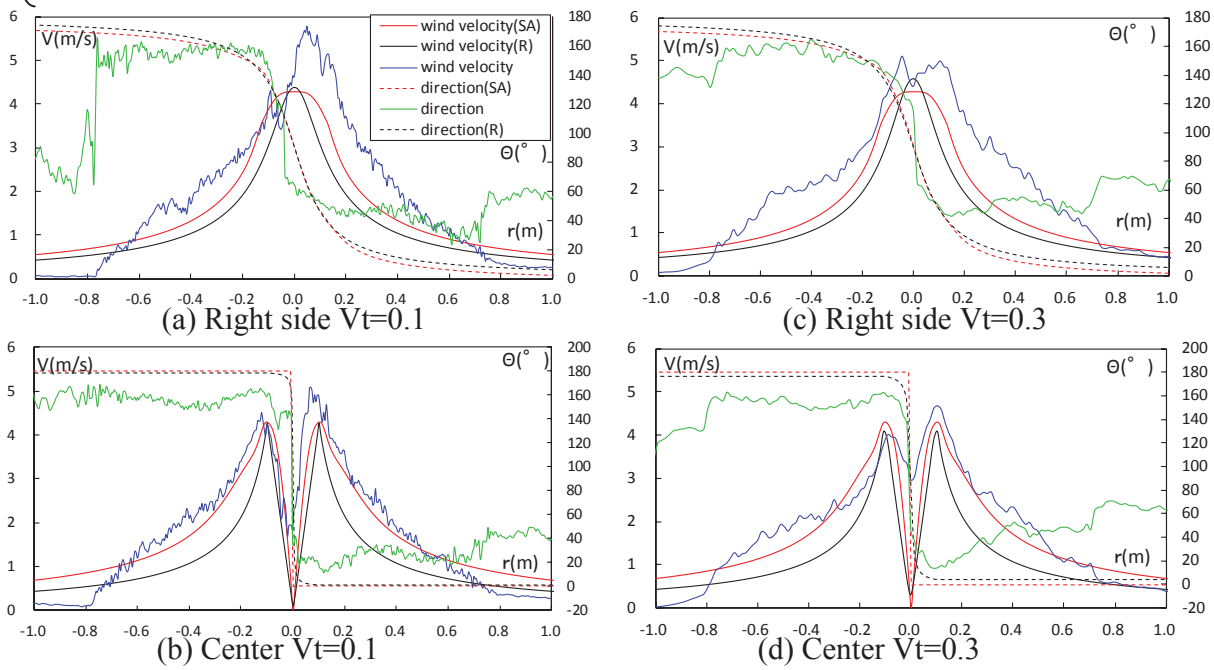

Figure 5 Time histories of measured wind speeds with the theoretical models

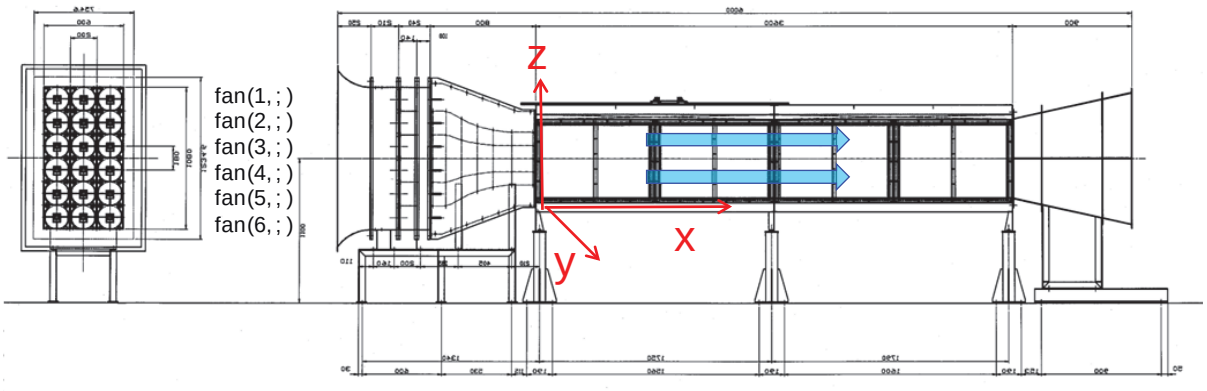

Figure 6 Diagram of multiple-fan wind tunnel and the coordinate system

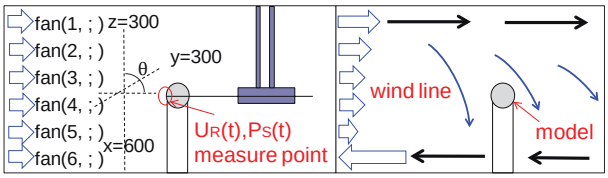

Figure 7 Mechanism of wind direction change and the measuring point

4 EXPERIMENT BY MULTIPLE-FAN WIND TUNNEL

4.1 *Simulation of Non-stationary Wind Flow based on Tornado Characteristics*

In order to investigate the non-stationary characteristics of a tornado, a multiple-fan wind tunnel is utilized to simulate part of the wind speed and direction profiles which are shown in Figure 5. A multiple-fan wind tunnel with 6×3 small fans is introduced in this research. As shown in Figure 6, fans are arranged in three vertical columns and each column contains six fans. Each fan can be actively controlled by computer independently. The rotation range of each fan is 0~3000rpm. By changing the input voltages of fans, non-stationary winds due to wind speed or direction changes can be simulated. To generate non-stationary wind flow caused by wind direction change, rotations of upper fans and lower fans can be controlled in the clockwise and counterclockwise direction. By balancing the rotation of these fans, stable wind direction change can be achieved. For the further measurement of wind speeds, the location with x=600mm, y=300mm, and z=300mm, is assumed as the measuring point. The mechanism of measurement is indicated as Figure 7.

Table 2 List of 9 types of non-stationary wind flows

stream type	⊿U(m/s)	⊿D(°)	⊿t(s)	remarks
st.1	–	–	–	stationary (0.9m/s)
st.2	–	–	–	stationary (2.2m/s)
st.3	1.2	–	1	velocity only
st.4	–	23.4	1	direction only
st.5	–	24.7	1	direction only (reverse)
st.6	1.5	22.0	1	vel & dir
st.7	1.2	18.8	1	vel & dir (reverse)
st.8	–	21.0	2	direction only
st.9	–	21.8	2	direction only (reverse)

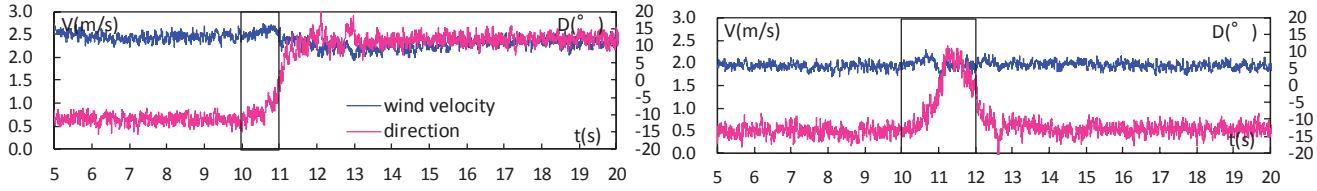

(a) Voltage of st.4

(b) Result of st.8

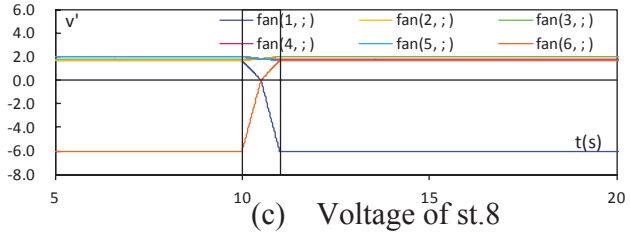

(c) Voltage of st.8

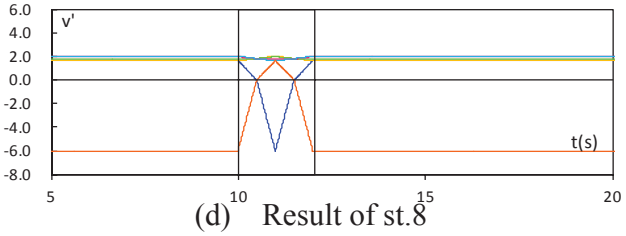

(d) Result of st.8

Figure 8 Examples of non-stationary wind flows, st4 and st8

To control each fan to generate non-stationary winds, it is necessary to vary the voltage in a short period. For the performance of fans in this research, the shortest period is 1 second. Further, to change the stationary status to non-stationary status (wind direction change here) which includes significant inverse rotation of fans, the wind speeds of fans are limited. In this research, the wind speed change is 50% of the maximum wind speed and 20° of the wind direction change.

Table 2 lists the simulated wind flow by multiple-fan wind tunnel. Wind flows st1 and st2 represent two stationary flows with two velocities; Wind flow st3 represents non-stationary flow with wind speed change of 1.2m/sec; Wind flows st4 and st5 represent two non-stationary flows with wind direction changes of 23.4° and 24.7° (reversely); Wind flows st6 and st7 represent non-stationary flows with both wind speed and direction changes; and Wind flows st8 and st9 represent the same condition as st4 and st5 but the period enlarges from 1 second to 2 seconds.
It is assumed that the downward wind direction change is indicated "-" and the upward direction is indicated "+". For non-stationary wind flows st3~st9, input voltages of fans arranged in the left column and right column are 60% of that in the middle column. Figure 8 shows the relationship of input voltage and wind speed and direction changes of st4 and st8 respectively. All the simulated wind flows remain uniform in the first 10 seconds and then start to change. An X type hot-wire anemometer is used for measurement in 1000Hz for 30 seconds. Ensample averaging is conducted by two records and moving averaging of every 200 samples is also executed.

4.2 *Distributions of Wind Speed and Direction*

In order to grasp the distributions of wind speed and direction of non-stationary wind flows inside the wind tunnel, a hot-wire anemometer is set at 25 grid measuring points shown as Figure 9. Interval of two neighboring measuring points is 25mm. Figure 10 shows the contour distributions of wind speed and direction of non-stationary st4. Each sub figure in Figure 10 represents the averaging result in certain period. It is indicated that the change of wind speed between two measuring points is less than 0.1m/sec and the wind direction change is quite stable.

4.3 *Wind Pressure Measurements on Square Prism Model*

As the results of circular prism model can eliminate the effect of velocity change ([7]), a square prism model is used to investigate the distributions of wind pressure coefficients due to non-stationary wind flow. The rotation of the square prism model is 5° and from 0°~45°. Wind pressures are recorded in 1000Hz for 30 seconds. Since the reference static wind pressure is different at different location in non-stationary wind flow, the reference static wind pressure measured on the wall of working sections of the wind tunnel is assumed for the calculation of wind pressure coefficients ([7]). The following equation is used for the definition of wind pressure coefficient.

$$C_p(t) = \frac{p'(t) - p_s(t)}{\frac{1}{2}\rho U_R(t)^2} \tag{2}$$

where $p'(t)$: measuring point; $p_s(t)$: reference static pressure; $U_R(t)$: basic wind speed.

It is known that the instantaneous maximum negative pressure around -1.2 is observed when the rotation angle is 15° ([3]). Figure 11 shows the dramatic large negative pressures when the wind direction changes in a very short period. Further, considering the wind direction change of 20° and the rotation angle of the model, the case of a 110° wind direction change can also be derived as shown in the diagram of Figure 12 and the time histories in Figure 13.

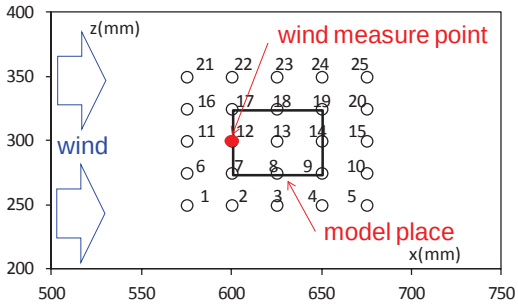

Figure 9 Measuring points inside the wind tunnel for wind velocity field

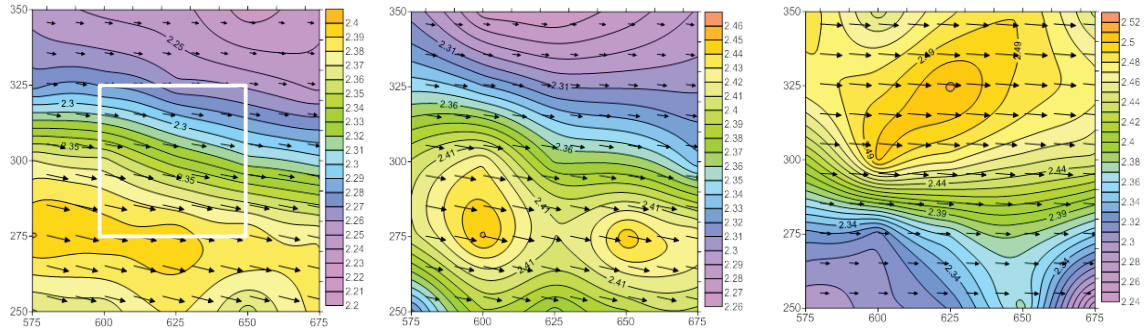

(a) 5-10s (b) 10-10.5s (c) 10.5-11s

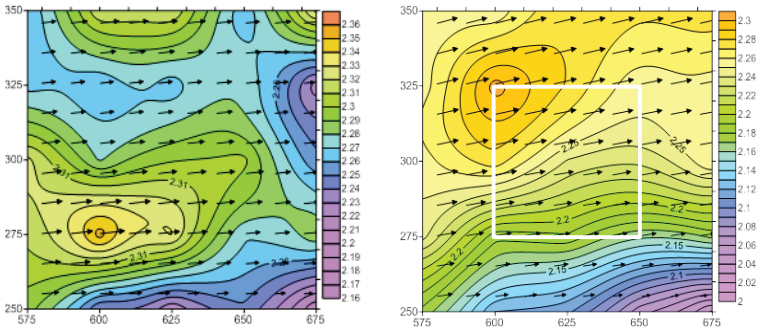

(d) 11-11.5s (e) 11.5-12s

Figure 10 Distributions of wind speed and direction of st4 non-stationary wind flow

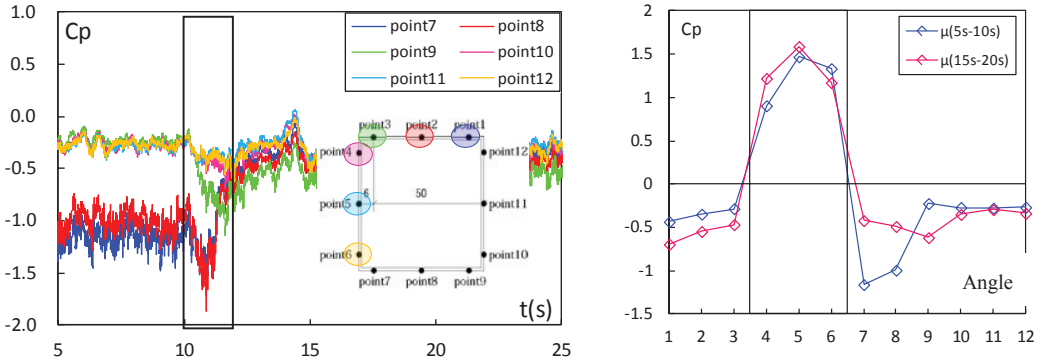

(a) Time-history (b) Average

Figure 11 Distribution of wind pressure coefficient of st5 flow with 5° rotation angle

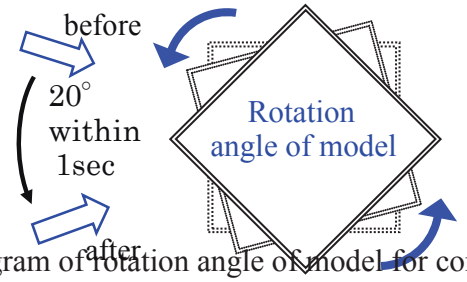

Figure 12 Diagram of rotation angle of model for continuous wind pressure coefficient measurements of 110°

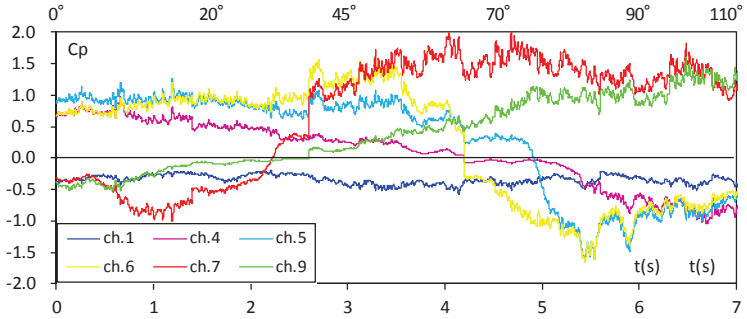

Figure 13 Derivation of wind pressure coefficients for each rotation angle for each pressure tubes

4.4 *Calculation of Wind Force Coefficients*

Wind force coefficients are derived by integrating wind pressures; however, due to the rotation of models, wind force coefficients are investigated in the x-direction and y-direction of the original model coordinates.

Figure 14 shows the wind force coefficient time histories in st4 flow for rotation angle of model equals 15° and 45°. It can be indicated clearly that instantaneous large wind forces shown in x-, y-, and torsion direction before and after the wind direction change. In this research, the shortest period is 1 second. Obvious overshoot phenomena cases are rare to investigate. Figure 15 shows respectively the obvious cases of wind speed change and wind direction change for st5 flow with 15° rotation angle and st4 flow with 10° rotation angle.

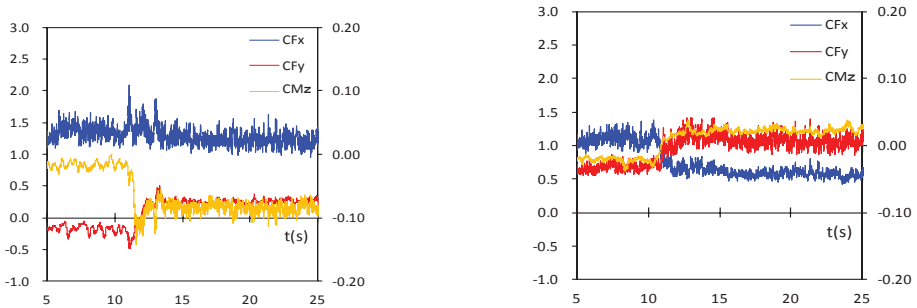

(a) Rotation angel 15° (b) Rotation angle 45°

Figure 14 Wind force coefficients of st4 with rotation angles

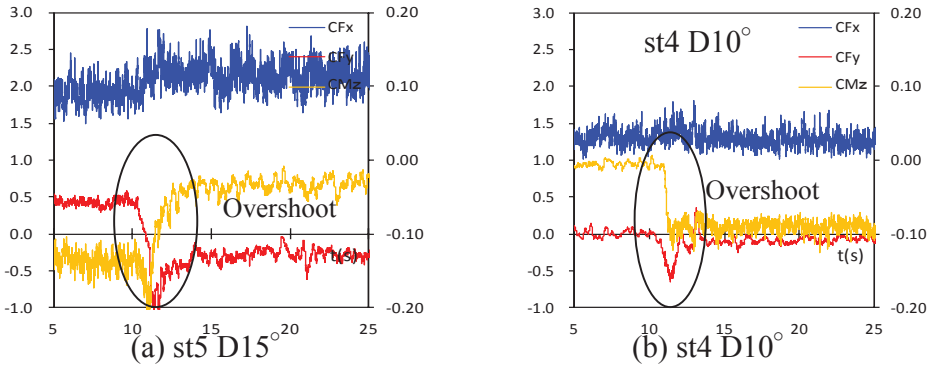

Figure 15 Observed examples of overshoot phenomena

5 CONCLUSIONS

Parameters of tornado model were first determined, based on statistical studies of recent tornado records in Japan. Then, tornado wind flow was simulated by tornado generator facilities and compared with theoretical tornado models. Nine types of non-stationary wind flows were simulated by multiple-fan wind tunnel for part of the tornado flow simulated in the generator facilities. Wind pressure measurements were then conducted under these types of non-stationary wind flows. From experimental results, it was indicated that large wind pressure coefficient around -1.2 were obtained when the rotation angle of model is 15° under wind direction change of 20° for a square prism model. And the overshoot phenomenon was also clearly observed. It is also indicated that a wind direction change of 110° can also be conducted by proper adjustment of rotation angle of the model and wind direction change. It may be anticipated that in the field scale, the effect on structures due to non-stationary wind flows is much more significant and essential.

ACKNOWLEDGEMENT

Grants-in-Aid for Scientific Research by JSPS are acknowledged for their financial support.

REFERENCES

1. M.E. Greenway, 1979, An analytical approach to wind velocity gust factors, J. Ind. Aerodyn., 5, p61-91
2. K. Idutu, J. Ikeuchi, T. Taniguchi, Y. Taniike, 2003, Study on the Wind Pressures due to Instantaneous Change of Wind Direction around a Cubic Model, Proceedings of AIJ Conference 2003 (in Japanese)
3. T. Ohkuma, J. Kanda, Y. Tamura, 2004, Wind Resistant Design of Structures, Kajima Co. (in Japanese)
4. A. Shakeel, Md. Ehtesham, 2009, Response of Transmission Towers Subjected to Tornado Loads, Proceedings of 7th Asia-Pacific Conference on Wind Engineering
5. J. Maeda, T. Takeuchi, 2010, Experimental Study of Unsteady Aerodynamic Forces – Properties of Unsteady Aerodynamic Forces under Wind Gust, Wind Engineers, JAWE, Vol.35, No.2 (in Japanese)
6. H. Kikitsu, P. P. Sarkar, Fred L. Haan, Jr., 2011, Experimental Study on Tornado-induced Loads on Low-rise Buildings Using a Large Tornado Simulator, Proceedings of ICWE13
7. R. Terai, J. Kanda, 2011, Non-stationary Wind Direction Simulation in Wind Tunnel with Computer-controlled Multiple Fans, Proceedings of ICWE13
8. Disaster on site report - On the gusty wind occurred in Tokunoshima, Kagoshima Prefecture on 18 November 2011, Naze observation station, Kagoshima regional meteorological agency (in Japanese)